Measurement 178 (2021) 109391

Contents lists available at ScienceDirect

Measurement

journal homepage: www.elsevier.com/locate/measurement

Compact Fabry-Perot microfiber interferometer temperature probe with closed end face

Jin Li (李晋) [a,b,c,*], Yan-nan Wang (王雁南) [a], Jun-tong Yang (杨俊彤) [a]

[a] College of Information Science and Engineering, Northeastern University, Shenyang 110819, China
[b] State Key Laboratory of Applied Optics, Changchun Institute of Optics, Fine Mechanics and Physics, Chinese Academy of Sciences, Changchun 130033, China
[c] Hebei Key Laboratory of Micro-Nano Precision Optical Sensing and Measurement Technology, Qinhuangdao, 066004, China

ARTICLE INFO

Keywords:
Microfiber sensor
Temperature sensor
Integrated optics
Fiber optics

ABSTRACT

In this paper, a Fabry-Pérot interferometer microprobe was constructed based on microfiber taper and hollow microfiber cone cavity. The interference cavity length of the Fabry-Pérot structure can be flexibly changed by moving the microfiber taper in the hollow microfiber. Polydimethylsiloxane solution was filled into the air cavity of the Fabry-Pérot interferometer to build a Fabry-Pérot temperature-sensitive microprobe with a stable structure by coaxially fixing the microfiber taper in the hollow fiber. The temperature sensitivity reached up to 2.41 nm/°C. The triple-repeated measurements and stability tests were experimentally verified with an excellent sensing performance. This small, compact, and end-sealed temperature-sensitive probe will push forward the development of wearable or implantable sensors.

1. Introduction

Temperature monitoring is essential in the fields of industrial production, biochemical reaction, and environmental safety [1,2]. Because of its small volume, light weight, electronic magnetic resistance, and high performance, the optical fiber temperature sensor occupies an irreplaceable position for determining the physical or chemical parameters in extreme and complex environments, such as small spaces and flammable and explosive environment [3]. In recent years, a variety of optical fiber temperature sensors have been demonstrated with the ultrahigh sensitivity and environmental adaptability. Fiber Bragg grating and long period grating become the most promising fiber sensors due to their good repeatability in preparation, stable structure, easy to demodulate and network. But the sensitivity was limited ~0.02 nm/°C, many sensitive material and complex encapsulation method were introduced to improve the sensing performance [4,5].

A special structure was designed to convert the temperature to the curve change of the polymer fiber, in which a temperature sensitivity of 1.04×10^{-3} °C^{-1} was obtained for the temperature range up to 110 °C [6]. Some materials with high thermo-optic or thermo-expansion coefficients were introduced to improve the sensing performance of optical fiber temperature sensors being filled into the fiber structure in the liquid form [7,8]. A D-shaped-hole, double-cladding fiber temperature sensor was proposed by employing an Au coating film and filling liquid to theoretically verify a high sensitivity of −3.635 nm/°C or even 42.99 nm/°C [9,10]. A higher sensitivity of −9.0 nm/°C was observed by combining a Sagnac loop interferometer with an indium-filled side-hole photonic crystal fiber (PCF) [11]. In another work, only a Sagnac loop was used to obtain a temperature sensitivity of 1.739 nm/°C [12]. Although PCF has the promising multi-core structures enabling the gas- or liquid-filling process, it also increases the manufacturing difficulty and cost of the device. Thermo-sensitive materials in solid form are desired to ensure the stability of temperature sensors.

By evaporating TiO_2 film on the end face of single mode fiber (SMF), splicing another cut of SMF, and encapsulating them by polydimethylsiloxane (PDMS) to fabricate a Fabry-Pérot microcavity, a temperature sensitivity of 0.13 dB/°C was experimentally demonstrated in the range of 22–60 °C [13]. Another similar temperature probe was designed to improve the response time (<0.09 s) and high-temperature (225 °C) working performance by splicing the multi-core fiber between SMFs [14]. The highest working temperature of >1500 °C was experimentally demonstrated by Tian et al. using a sapphire fiber extrinsic Fabry-Pérot interferometer [15]. Fabry-Perot interferometer can also be formed by fiber Bragg grating mirrors, resulting in the temperature resolution of 0.005 °C during 25–170 °C [16]. The composite fiber structures have the potential application for measuring muti-parameters

* Corresponding author at: College of Information Science and Engineering, Northeastern University, Shenyang 110819, China.
E-mail addresses: lijin@ise.neu.edu.cn (J. Li (李晋)), 2597831105@qq.com (Y.-n. Wang (王雁南)), yangjuntongjiayou@163.com (J.-t. Yang (杨俊彤)).

https://doi.org/10.1016/j.measurement.2021.109391
Received 24 August 2020; Received in revised form 23 March 2021; Accepted 6 April 2021
Available online 18 April 2021

at the same time and solving the problem of temperature cross sensitive. Generally, the high-temperature working characteristics depend on the special processed optical fiber structures without the assistance of sensitive materials. These Fabry-Perot structures were emerge as the air holes on or through the optical fiber machined by the fs laser etching technology [17,18]; but the high-sensitivity characteristics are rely on sensitive materials, such as PDMS, which have been experimentally demonstrated in our previous works [19]. However, for a Fabry-Pérot structure with an open cavity, the temperature sensing characteristics are easily affected by the ambient humidity [20]. High resolution is required for the temperature precise controlling in the marine environment research, the chemical reaction of industrial manufacturing, the thermal deformation of optical system and the resource optimizing of precision agriculture [21].

In this paper, a reflected Fabry-Pérot interferometer temperature sensor with a closed end is proposed. The temperature sensitivity was improved by the thermo-expansion and elastic-optic effects of the solidified PDMS filled in the air cavity of the Fabry-Pérot structure.

2. Microfiber Fabry-Perot interferometer temperature probe preparation

The structure of the Fabry-Pérot interference sensor designed and studied in this work is mainly composed of a single-mode microfiber taper and a hollow-core fiber with a melted conical air cavity at its end. This structure is packaged with temperature-sensitive material, i.e., PDMS. The fabrication process mainly includes the fabrication of the microfiber taper, preparation of the conical air cavity at the end of the hollow fiber, the optimization of cavity length, and PDMS filling.

The microfiber taper was made by the flame-scanning melt-drawing method using a multi-functional fiber-stretching machine (IPCS-5000-SMT). A microfiber with specific diameter and smooth surface can be obtained by controlling the temperature of hydrogen oxygen flame, heating region (scanning heating or fixed-point heating), and drawing speed. Then, the fixed-point cutting and fiber end-face observation were completed with the help of a homemade microscope-micromanipulation system. First, the hollow-core fiber was selected, having the outer diameter of 162 μm and the inner diameter of 100 μm (TSP160100, Polymicro). After removing the coating layer, the hollow-core fiber was placed into a fusion machine (Furukawa S178), in which the manual fusion model was used to adjust the discharge position at one end of the hollow-core fiber and discharge to obtain the conical cavity. The other end of the hollow-core fiber was cut to the proper length to facilitate the insertion of the microfiber taper.

The conical cavity of the hollow-core fiber was filled with PDMS. After the solidification of the PDMS, the microfiber was fixed consistently with the central axis of the hollow-core fiber to complete the Fabry-Pérot interferometer. When the temperature changes, its cavity length will change due to the thermo-optic and elastic-optic effects, and the optical path difference will result in the shift of the interference spectrum. Therefore, the temperature can be demodulated by tracing the shift of the specified resonance peaks.

To select the appropriate diameter and cavity length, four sensing structures with diameters of 20, 28, 36, and 44 μm were fabricated. The cavity length can be flexibly adjusted before PDMS solidification by moving the microfiber taper in the hollow core fiber. It was fixed at 30 μm to explore the impact of microfiber diameter on the interference spectrum. By analyzing the reflection spectra of the Fabry-Pérot structures with different microfiber diameters, as shown in Fig. 1, the diameter parameter was optimized by comparing the corresponding peak (dip) intensity, period number, and extinction ratio. The comparison results for the period numbers and extinction ratio (i.e., the ratio of the highest peak power to the lowest peak power) of the Fabry-Pérot reflection spectrum reveals that the interference spectrum exhibits significant clutter when the microfiber diameters are 20 and 28 μm. Furthermore, it is clear that the intensity (dB) varies with diameter

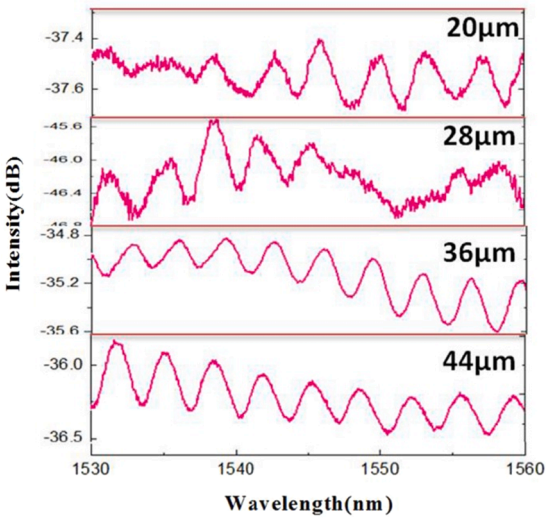

Fig. 1. Interference spectra for Fabry-Perot structure with a fixed cavity length of 30 μm and microfiber diameters of 20 μm, 28 μm, 36 μm and 44 μm, respectively.

inconsistently. This power uncertainty phenomenon is mainly affected by the end-face flatness of microfiber, which has a large randomness during the process cutting, because the fiber material becomes extremely brittle after the heating-melting treatment. The thinner microfiber tapers excited more complex optical modes, leading to loss or enhancement of some optical signals with special wavelengths in the reflection spectrum. When the diameters of the tapered fiber were 36 and 44 μm, the reflection spectrum quality and extinction became better. When a 44-μm microfiber taper was used, the extinction ratio and the spectral period numbers increase with cavity length (from 30, 60, and 90 μm to 120 μm). For the cavity length of 30 μm, the free spectrum range (FSR) was too wide, and only one resonance peak exists during the wavelength range of light source. It is difficult to determine the specific wavelength value of the peak value due to the wide pulse. Moreover, when the cavity length was longer than 60 μm, the period numbers were too large [that is, the FSR became narrowed], and the extinction ratio was worse. The final structural parameters for the microfiber diameter and cavity length were set as 50 and 40 μm, respectively. The fringe contrast is not high compared with that of hollow Fabry-Perot interferometer due to the light reflection loss on the surface of the two reflectors. It is promising to be improved by optimize the fabrication process of hollow fiber cone and microfiber taper to obtain a flatter surface.

The temperature-sensitive material, i.e., PDMS, was used to encapsulate the Fabry-Pérot structure. The PDMS solution was obtained by mixing main and curing agents at a ratio of 10:1 and was then filled into the conical air cavity of the hollow-core fiber. After the PDMS became solidified, the microfiber taper was fixed and lined consistent with the central axis of the hollow-core fiber to ensure the quality of the interference spectrum. The microfiber Fabry-Pérot temperature probe was obtained with a fixed cavity length. During the fabrication process, the cavity length was precisely controlled by moving the microfiber taper in hollow fiber using our home-made micromanipulation system. The PDMS solution can be solidified quickly by placing it in a thermostat and heating at 80 °C for 1 h

3. Temperature sensing experiment and results analysis

As shown in Fig. 2, the experimental system mainly comprises an amplified spontaneous emission (ASE) light source (Golight 1550-nm ASE; wavelength, 1520–1610 nm), circulator, thermostat (Boxun BGZ-30; temperature range, room temperature to 250 °C), and

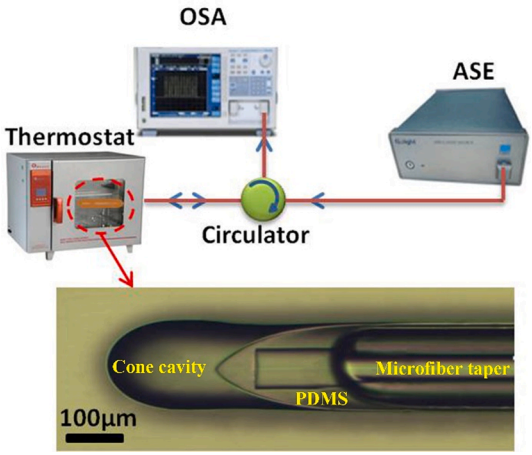

Fig. 2. Schematic diagram of experiment and microscope photo of temperature probe.

spectrometer (Yokogawa AQ6370; resolution, 20 pm). The temperature-sensor probe was placed in the thermostat.

When the temperature rises or falls, the Fabry-Pérot cavity length and refractive index of the fiber core changes, and the spectrum moves to the right or left accordingly. The single-peak demodulation method was used to trace one interference dip of the spectra in the experiment to determine the relationship of the temperature as a function of wavelength location, as shown in Fig. 3, where the temperature changes from 30 °C to 34 °C.

With temperature increasing, the reflectance spectrum red shifted as a whole with the rate of ~2.4 nm/°C. Because of the high temperature sensitivity, the temperature sensing performance will only be experimental demonstrated first during a short range. Since the FSR of the interference spectrum was less than 6 nm, the wavelength position of the specific interference peak (dip) must be selected and tracked to plot the temperature-response curve. When a characteristic peak (dip) value was tracked continuously over the entire wavelength range of the light source (90 nm), the continuous temperature change for ~30 °C can be determined, but it will take too long time for the increasing and decreasing process of temperature. In this experiment, the temperature range from 25 °C to 35 °C was calibrated by tracing one interference dip. The temperature sensor probe was heated first from 25 °C to 35 °C, and then cooled from 35 °C to 25 °C, with the corresponding sensitivities of 2.41 nm/°C and 2.42 nm/°C, respectively.

To verify the repeatability of the temperature sensor, three rounds of the increasing–decreasing process between 25 °C and 35 °C was experimentally carried out. As indicated in Fig. 4, the fitting curve reveals that the interference spectrum undergoes a small drift during the temperature-decrease process. It is likely that the temperature of the sensor-probe position will be lower than the display temperature of the thermostat when it is cooled by the blast flow. However, the three fitting curves exhibit little difference in either sensitivity (Increasing process-IP, <0.078 nm/°C; Decreasing process-DP, <0.243 nm/°C) or return error (~0.469 nm).

To further test the stability of the sensor, the temperature was frequency-changed between 30 °C and 33 °C to observe the fluctuation of the wavelength location of interference dip, as shown in Fig. 5.

As both the temperature increasing and decreasing processes were very slow, only the stability of the wavelength location for the fixed temperature is demonstrated here. The experimental results cannot indicate either response or recovery time for the temperature sensor. For the fixed-temperature environment, the overall performance of the sensor was stable, with a power-fluctuation range of less than 0.34 nm. For most of the FP interferometer sensors, the cross sensitivity between the parameters must be discussed. Because most of Fabry-Pérot interferometers have an open cavity structure or a closed film that directly contacts with the external environment [22,23]. In addition to being sensitive to temperature, the sensitive materials or Fabry-Pérot structures (for example, the encapsulated film) are susceptible to humidity, pressure, and vibration [24]. The proposed FP interferometer is completely encapsulated in the tapered hollow fiber. The microfiber is completely fixed by PDMS. Therefore, the cross sensitivity of other parameters to temperature can be ignored in this experiment.

Theoretically, the working range of the temperature sensor as designed will be −50 °C to 200 °C, only limited by the temperature tolerance range of PDMS. The thermostat temperature can be controlled from room temperature to 250 °C. Therefore, the temperature-sensing performance of the proposed sensor was further experimentally demonstrated for the higher temperature. Fig. 6 show the temperature-sensing characteristic curves in the ranges of 25–125 °C. Because of the wide temperature range, it is necessary to select different characteristic interference peaks (dips) to calibrate the sensing performance in different intervals to complete the temperature measurement in the whole temperature range, where the corresponding resonance wavelength will be different. Therefore, in Fig. 6, the relative wavelength shift of the interference peaks (dips) was used to explain its depending relationship with temperature change.

The sensitivity in the higher temperature region is slightly lower than that in the lower one. The sensor system exhibits good stability and sensing performance. When the temperature is over 115 °C, the sensitivity drops rapidly, and more modes turn out in the interference spectrum, which will seriously interfere with the interference-dip tracking

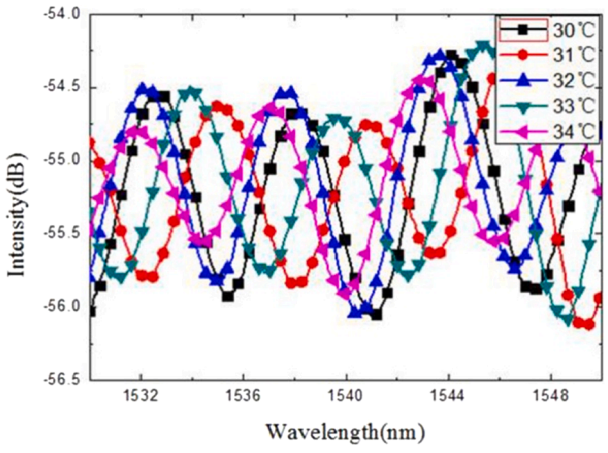

Fig. 3. Reflected spectrum changes as a function of temperature increasing from 30 °C to 34 °C.

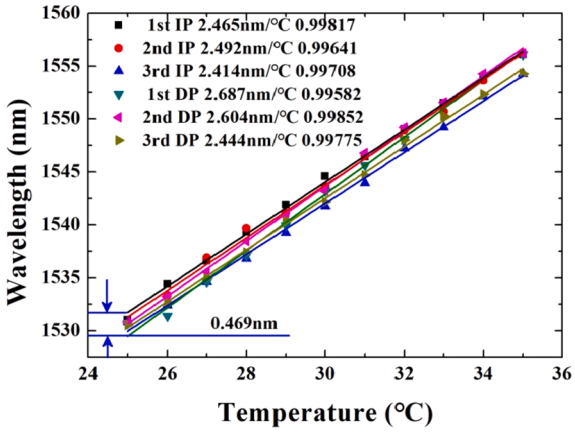

Fig. 4. Triple temperature-sensing characteristic curves of microfiber Fabry-Pérot sensor in increasing–decreasing process between 25 °C and 35 °C.

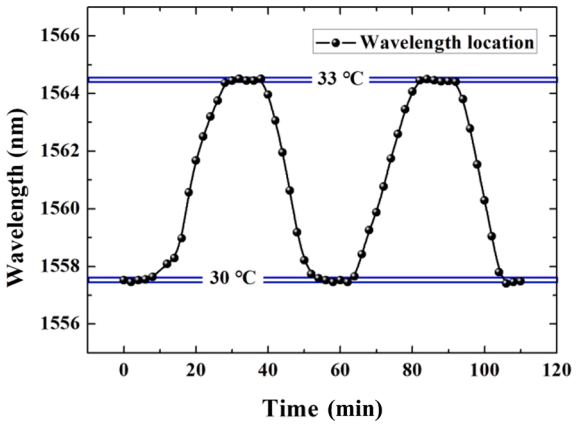

Fig. 5. Stability curves of microfiber temperature sensor at fixed temperature.

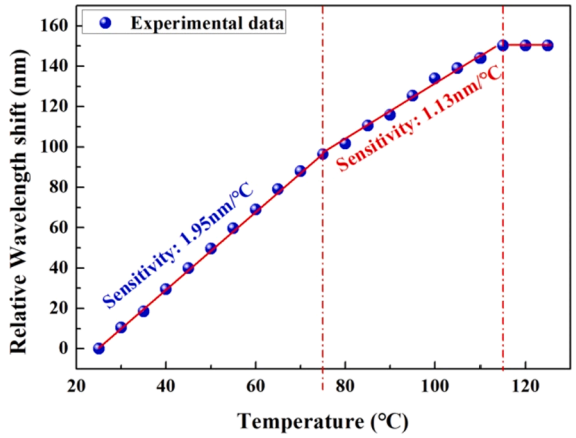

Fig. 6. Temperature-sensing curves in a wide temperature range.

and temperature measurement. This can be attributed to the insignificant thermal expansion of PDMS in the higher temperature range. Furthermore, in addition to the Fabry-Pérot cavity, the PDMS also be used to fix the microfiber taper, caused that the linear expansion of the cavity was limited. The structure of the sensor must be optimized for a larger operating range. Therefore, the working range of the proposed microfiber Fabry-Pérot temperature sensor can be finally determined from 25 °C to 115 °C.

4. Conclusions

A microfiber Fabry-Pérot structure was fabricated by inserting a microfiber taper into a micrometer-sized hollow fiber with a closed end. The microfiber end and cone cavity surface of the hollow fiber were used as the two reflectors of the Fabry-Pérot interference structure. The interference-spectrum quality was greatly affected by the diameter of the microfiber taper and geometry angle of the conical air cavity. An overly thin microfiber will reduce the interference light intensity and may play the role of an optical filter. The cone angle and external geometric contour of the conical air cavity may introduce the resonance effect of whisper gallery modes. By filling the air cavity with PDMS solution and curing, the proposed temperature sensor was experimentally demonstrated with a high sensitivity. Tiny changes of temperature acts on the PDMS, causing the change of its equivalent refractive index and volume, and resulting in the change of the cavity length of the Fabry-Pérot interferometer. A temperature sensitivity of >2.4 nm/°C was obtained by tracing the wavelength location of the special resonance dip. However, the results of repeatability and stability experiments indicate a significant fluctuation of ~0.469 nm and ~0.253 nm, respectively, which can be partially attributed to the temperature-control accuracy of the blast drying oven. The temperature-measurement range was finally experimentally demonstrated to range from 25 °C to 115 °C with good stability and repeatability.

CRediT authorship contribution statement

Jin Li (李晋): Supervision, Funding acquisition, Writing - review & editing. **Yan-nan Wang (王雁南):** Writing - original draft, Data curation. **Jun-tong Yang (杨俊彤):** Conceptualization, Writing - original draft, Visualization.

Declaration of Competing Interest

The authors declare that they have no known competing financial interests or personal relationships that could have appeared to influence the work reported in this paper.

Acknowledgement

This work was supported by the National Key R&D Program of China (2019YFB2006001), Fundamental Research Funds for Central Universities (N2004007), and Hebei Natural Science Foundation (F2020501040).

References

[1] Q. Li, L.N. Zhang, X.M. Tao, X. Ding, Review of flexible temperature sensing networks for wearable physiological monitoring, Adv. Healthc. Mater. 6 (12) (2017) 1601371.
[2] M.S. Yoon, S. Park, Y.G. Han, Simultaneous measurement of strain and temperature by using a micro-tapered fiber grating, J. Lightw. Technol. 30 (8) (2011) 1156–1160.
[3] J. Li, H. Yan, H. Dang, et al., Structure design and application of hollow core microstructured optical fiber gas sensor: A review, Opt. Laser Technol. 135 (2021) 106658.
[4] R. Oliveira, L. Bilro, T.H.R. Marques, C.M.B. Cordeiro, R. Nogueira, Simultaneous detection of humidity and temperature through an adhesive based Fabry-Perot cavity combined with polymer fiber Bragg grating, Opt. Laser. Eng. 114 (2019) 37–43.
[5] C. Du, Q. Wang, Y. Zhao, Electrically tunable long period gratings temperature sensor based on liquid crystal infiltrated photonic crystal fibers, Sensor Actuat. A 278 (2018) 78–84.
[6] A. Leal, A. Frizera-Neto, C. Marques, M.J. Pontes, A polymer optical fiber temperature sensor based on material features, Sensors-Basel 18 (1) (2018) 301.
[7] J. Li, Q. Nie, L.T. Gai, H.Y. Li, H.F. Hu, Highly sensitive temperature sensing probe based on deviation S-shaped microfiber, J. Lightw. Technol. 35 (17) (2017) 3699–3704.
[8] X.C. Yang, Y. Lu, B.L. Liu, J.Q. Yao, Temperature sensor based on photonic crystal fiber filled with liquid and silver nanowires, Ieee Photonics J. 8 (3) (2016) 1–9.
[9] S.J. Weng, L. Pei, J.S. Wang, T.G. Ning, J. Li, High sensitivity D-shaped hole fiber temperature sensor based on surface plasmon resonance with liquid filling, Photonics Res. 2 (2017) 103–107.
[10] N. Ayyanar, R.V.J. Raja, D. Vigneswaran, B. Lakshmi, M. Sumathi, K. Porsezian, Highly efficient compact temperature sensor using liquid infiltrated asymmetric dual elliptical core photonic crystal fiber, Opt. Mater. 64 (2017) 574–582.
[11] E. Reyes-Vera, C.M.B. Cordeiro, P. Torres, Highly sensitive temperature sensor using a Sagnac loop interferometer based on a side-hole photonic crystal fiber filled with metal, Appl. Opt. 56 (2) (2017) 156–162.
[12] J. Shi, Y.Y. Wang, D.G. Xu, H.W. Zhang, G.H. Su, L.C. Duan, C. Yan, D.X. Yan, S. J. Fu, J.Q. Yao, Temperature sensor based on fiber ring laser with Sagnac loop, Ieee Photonic. Tech. L. 28 (7) (2016) 794–797.
[13] I. Hernandez-Romano, M.A. Cruz-Garcia, C. Moreno-Hernandez, D. Monzon-Hernandez, E.O. Lopez-Figueroa, O.E. Paredes-Gallardo, M. Torres-Cisneros, J. Villatoro, Optical fiber temperature sensor based on a microcavity with polymer overlay, Opt. Express 24 (5) (2016) 5654–5661.
[14] M.D. Wales, P. Clark, K. Thompson, Z. Wilson, J. Wilson, C. Adams, Multicore fiber temperature sensor with fast response times, OSA Continuum. 1 (2) (2018) 764–771.
[15] Z.P. Tian, Z.H. Yu, B. Liu, A.B. Wang, Sourceless optical fiber high temperature sensor, Opt. Lett. 41 (2) (2016) 195–198.
[16] Xiaoke Wan, Henry F. Taylor, Intrinsic fiber Fabry-Perot temperature sensor with fiber Bragg grating mirrors, Opt. Lett. 27 (16) (2002) 1388–1390.
[17] P.C. Chen, X.W. Shu, Refractive-index-modified-dot Fabry-Perot fiber probe fabricated by femtosecond laser for high-temperature sensing, Opt. Express 26 (5) (2018) 5292–5299.

[18] T. Wei, Y.K. Han, H.L. Tsai, H. Xiao, Miniaturized fiber inline Fabry-Perot interferometer fabricated with a femtosecond laser, Opt. Lett. 33 (6) (2008) 536–538.
[19] Z.B. Li, Y. Zhang, C.Q. Ren, Z.Q. Sui, J. Li, A high sensitivity temperature sensing probe based on microfiber Fabry-Perot interference, Sensors-Basel 19 (8) (1819) 2019.
[20] S.Q. Liu, Y.K. Ji, J. Yang, W.M. Sun, H.Y. Li, Nafion film temperature/humidity sensing based on optical fiber Fabry-Perot interference, Sensor. Actuat. A-Phys. 269 (2018) 313–321.
[21] X.D. Wang, O.S. Wolfbeis, R.J. Meier, Luminescent probes and sensors for temperature, Chem. Soc. Rev. 42 (2013) 7834–7869.
[22] S. Pevec, D. Donlagic, Miniature all-fiber Fabry-Perot sensor for simultaneous measurement of pressure and temperature, Appl. Opt. 51 (19) (2012) 4536–4541.
[23] Y. Gong, C.B. Yu, T.T. Wang, X.P. Liu, Y. Wu, Y.J. Rao, M.L. Zhang, H.J. Wu, X. X. Chen, G.D. Peng, Highly sensitive force sensor based on optical microfiber asymmetrical Fabry-Perot interferometer, Opt. Express 22 (3) (2014) 3578–3584.
[24] Y. Gong, Y. Guo, Y.J. Rao, T. Zhao, Y. Wu, Fiber-Optic Fabry-Pérot Sensor Based on Periodic Focusing Effect of Graded-Index Multimode Fibers, Ieee Photonic. Tech. L. 22 (23) (2010) 1708–1710.